FATIGUE CRACK GROWTH BEHAVIOR OF A MICROALLOYED STEEL WITH MULTIPHASE MICROSTRUCTURES

Denise F. Laurito, denisefl@ppgem.eel.usp.br
Carlos Antonio R. P. Baptista, baptista@demar.eel.usp.br
EEL/USP – Escola de Engenharia de Lorena da Universidade de São Paulo
Polo Urbo-Industrial, Gleba AI-6, Lorena/SP

Antonio J. Abdalla, abdalla@ieav.cta.br
IEAv/CTA – Instituto de Estudos Avançados, Comando-Geral de Tecnologia Aeroespacial
São José dos Campos/SP

Marcelo A. S. Torres, mastorres@uol.com.br
FEG/UNESP – Faculdade de Engenharia do campus de Guaratinguetá da Universidade Estadual Paulista
Guaratinguetá/SP

Abstract. *Microalloyed steels are a class of HSLA steels with low or medium carbon content and small additions of alloying elements such as Mn, Nb, Mo, V and Ti. They have been developed in order to replace the conventional quenched and tempered steels. A variety of microstructures in microalloyed steels can be obtained depending on the deformation temperature, cooling rate and chemical composition. Isothermal transformation on these materials, with various temperatures and holding times, produces multiphase microstructures with different amounts of ferrite, martensite, bainite and retained austenite. These different phases, with distinct morphologies, are determinant of the mechanical behavior of the steel and can, for instance, affect crack closure or promote crack shielding, thus resulting in changes on its propagation rate under cyclic loading. The aim of the present work is to evaluate the effects of microstructure on the tensile strength and fatigue crack growth behaviour of a 0.08%C-1,5%Mn (wt. pct.) microalloyed steel, recently developed by CSN (Companhia Siderúrgica Nacional) under the designation of B550. This steel is being considered as a promising alternative to replace low carbon steel in wheel components for the automotive industry. Various microstructural conditions were obtained by means of inter-critical and isothermal heat treatments followed by water quench, in which the material samples were kept at the temperatures of 800, 950 and 1200°C. The as-received material condition was also employed for comparison. The crack propagation test results were summarized in terms of FCG rate (da/dN) versus stress intensity factor range (ΔK) curves. In order to describe the FCG behavior, two models were tested: the conventional Paris equation and a new exponential equation developed for materials showing non-linear FCG behavior. The results allowed correlating the tensile properties and crack growth resistance to the microstructural features. Moreover, it is shown that the Paris regime FCG curves of the dual and multiphase microstructural conditions present crack growth transitions that are better modeled by dividing them in two regions.*

Keywords*: microalloyed steels, heat treatment, fatigue crack growth*

1. INTRODUCTION

The need for reduction of the vehicles' weight lead to the development of steels with improved chemical composition and microstructure. The mechanical properties of these new materials, which include the high strength and low alloy (HSLA) steels and the microalloyed steels, are more favorable both to manufacturing and service performance of automotive components. These steels have low or medium carbon content and small additions of alloy elements such as Mn, Nb, Mo, V and Ti. A variety of microstructures in microalloyed steels can be obtained depending on the deformation temperature, cooling rate and the chemical composition (Naylor, 1998; ASM, 1999; Matlock *et al.*, 2001).

Microalloying elements are added mainly to control the austenitic grain size of the reheating, to retard the recrystallization of austenite and to promote precipitation hardening. Elements such as Nb and Ti facilitate grain refinement by means of the precipitation and anchoring of solute in austenite and contribute to increase the strength by precipitation in ferrite during and after the austenite→ferrite transformation (Elisei *et al.*, 2006).

On the other hand, the research involving the transformation of phases by means of inter-critical and isothermal heat treatments have intensified, with promising results given by the dual phase steels (Abdalla *et al.*, 2004). These are characterized by microstructures consisting of a dispersion of hard martensite particles in a soft ferrite matrix. Due to its combination of high strength, good ductility and continuous yielding, dual phase steels have been considered to be ideal for the production of automobile components that require good formability (Liang *et al.*, 2008). Microalloyed steels can also be heat treated in order to obtain dual phase and multiphase microstructures.

The strength, ductility and fatigue resistance of steels can be related to their microstructural aspects. Tayanç *et al.* (2007) investigated the effect of carbon content and martensite volume fraction on the fatigue behavior strength of dual phase steels with carbon content between 0.085% and 0.3% (wt. pct.). They observed that dual phase steels show better fatigue properties than the as received steels. Moreover, an optimum heat treatment temperature preceding water quenching was found to exist for the studied steels, with respect to tensile strength. Baptista *et al.* (1994) investigated the fatigue crack growth (FCG) behavior of dual phase steels and found that a higher tensile strength corresponds to

lower FCG resistance. Suzuki and McEvily (1979) obtained FCG curves for dual phase steels presenting duplex microstructures with distinct phase morphologies. They observed that not only the martensite fraction volume, but also its morphology, can significantly affect the FCG behavior.

The aim of the present work was to evaluate the effects of microstructure on the tensile strength and fatigue crack growth behaviour of a 0.08%C-1,5%Mn (wt. pct.) microalloyed steel, recently developed by CSN (Companhia Siderúrgica Nacional) under the designation of B550. This steel is being considered as a promising alternative to replace a low carbon steel in wheel components for the automotive industry. Distinct microstructural conditions were obtained by means of inter-critical and isothermal heat treatments followed by water quench, in which the material samples were kept at the temperatures of 800, 950 and 1200^{o}C. The as-received (hot-rolled) material condition was also employed for comparison. The crack propagation test results were summarized in terms of FCG rate (da/dN) versus stress intensity factor range (ΔK) curves. In order to describe the FCG behavior, two models were tested: the conventional Paris equation (Paris and Erdogan, 1963) and a new exponential equation developed for materials showing non-linear FCG behavior (Adib and Baptista, 2007). The results allowed correlating the tensile properties and crack growth resistance to the microstructural features. Moreover, it is shown that the Paris regime FCG curves of the dual and multiphase microstructural conditions present crack growth transitions that are better modeled by dividing them in two regions.

2. EXPERIMENTAL PROCEDURE

The material used in this study was a commercial grade low carbon microalloyed steel, developed by CSN under the designation of B550. The chemical composition of this steel is given in Tab. 1. The material was received as hot rolled plates with 5 mm in thickness, from which tensile and fatigue specimens were machined. These specimens were divided in four lots; the first one remained in the “as received” (AR) condition. The others were hold in furnace at 800, 950 and 1200°C for 30 min, and then the specimens were quenched directly into cold water. After heat treatment, cross-section of samples were polished, etched and observed under light and scanning electron microscope (SEM) in order to reveal their microstructures. Three distinct etching procedures were adopted: 2% nital, 10% sodium metabisulphite and a combination of them.

Table 1. Chemical composition of B550 steel.

Element	C	Mn	P	S	Si	Cu	Ni	Cr
wt. %	0.085	1.169	0.017	0.005	0.053	0.007	0.008	0.016
Element	Mo	Sn	Al	N	Nb	V	Ti	B
wt. %	0.005	0.003	0.021	0.0055	0.035	0.003	0.013	0.001

The tensile and fatigue crack growth tests were conducted at room temperature in laboratory air using a MTS 810.23m servo-hydraulic machine with 250 kN capacity. For the tensile tests, small size specimens (6 mm in width and gage length of 30 mm) and a constant crosshead speed of 0.5 mm/min were employed.

Compact tension specimens, cut in the LT orientation, were adopted for the FCG tests. These were performed with constant load amplitude under force control at load ratio (min/max) R = 0.1. The test frequency was kept constant at 10 Hz and the loading waveform was sinusoidal. The compliance method of crack length monitoring was used during the tests and the five point incremental polynomial technique was employed for computing the crack growth rate. All of the experimental and numerical procedures were in conformity with the standard practice for Measurement of Fatigue Crack Growth Rates (ASTM E647-95a). The crack propagation test results were summarized in terms of FCG rate (da/dN) versus stress intensity factor range (ΔK) curves.

3. RESULTS AND DISCUSSION

The obtained results are summarized in three sections: microstructural analysis, tensile propertied and fatigue crack growth behavior. In these analyses, the material in the “as received” condition is referred as AR; the remaining material conditions are designated by WQ (from “water quench”) followed by a number representing the soaking temperature, i.e., WQ800, WQ950 and WQ1200.

3.1. Microstructural analysis

It can be seen if Fig. 1a that the AR material presents fine grained microstructure with polygonal morphology. The microalloying elements Nb, V and Ti contribute to the formation of small size grains in the hot rolled steel. Figure 1b (nital etching) shows that the main phases in this material are perlite (dark) and ferrite (bright). The same material condition was also etched in an aqueous solution of sodium metabisulphite in order to reveal the presence of retained

austenite. However it was not possible to detect this phase, which means that its amount in the AR condition is negligible.

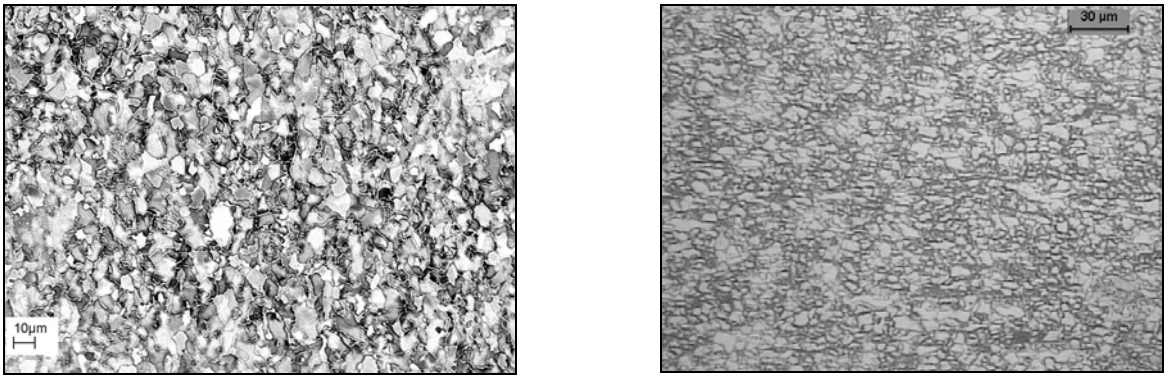

(a) (b)

Figure 1. B550 steel, AR condition. (a) SEM micrography showing grain refinement; (b) optical micrography revealing the grain boundaries and phases: perlite (dark) and ferrite (etchant: 2% nital).

The microstructure of WQ800 condition, shown in Fig. 2, presented changes in grain size compared to the AR material. By heating the steel to the intercritical region (800°C), two phenomena occur: the formation of carbon-enriched austenite and the growth of non-transformed ferrite grains. The austenite grains in equilibrium with the remaining ferrite are small and in lower amount due to the low carbon content of the alloy. After quenching, austenite is transformed in a second, harder phase (martensite and/or bainite) spread over the ferrite matrix, resulting in a typical dual phase steel microstructure. In Fig. 2b, the same microstructure is revealed by sodium metabissulphite etching. In this case, the small white globular areas correspond to retained austenite, indicating that part of the austenite did not transform, due to the severity of the water quench.

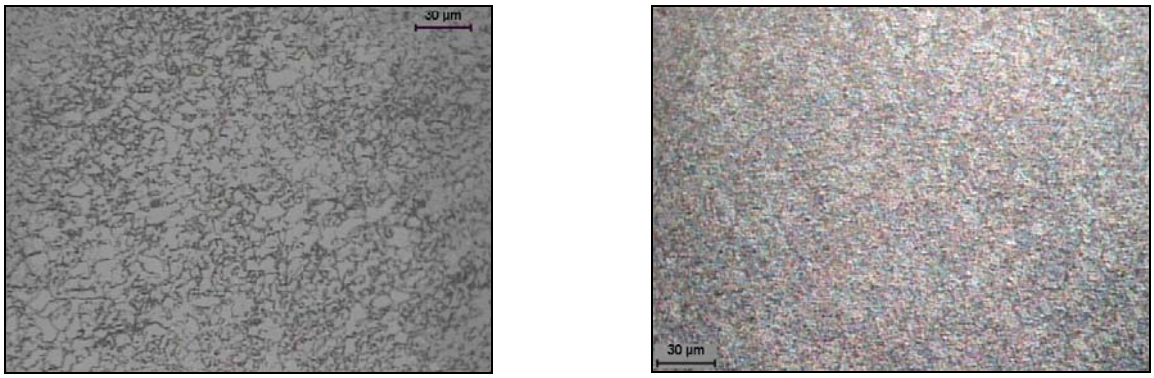

(a) (b)

Figure 2. B550 steel, WQ800 condition, optical micrographies. (a) Dual phase structure (etchant: 2% nital); (b) retained austenite, white phase (etchant: 10% sodium metabissulphite).

It can be seen in Fig. 3a that the water quench from a total austenitization temperature (950°C) brought deeper microstructural changes to this steel. The polygonal aspect of the grains was reduced, the soft phase (ferrite) became more acicular and the amount of the second phase (martensite/bainite) is increased. The overall microstructure is still refined. Liang *et al.* (2008) observed a similar microstructure as a result of water quenching from the austenitic region. The micrography obtained with sodium metabisulphite etching, Fig. 3b, shows that the amount of retained austenite (white phase) is increased for this soaking temperature.

The microstructure of WQ1200 condition is shown in Fig. 4. In this case, the blue-tinted phase (martensite), sprinkled with a white phase (retained austenite), has a tendency to surround the ferritic phase (pale brown) like a net, see Fig. 4a. It can be seen in Fig. 4b the ripped up morphology of the transformed phases, indicating that shearing events occurred during transformation. This occurrence is well known for low carbon (less than 0.6 wt. pct.) steels.

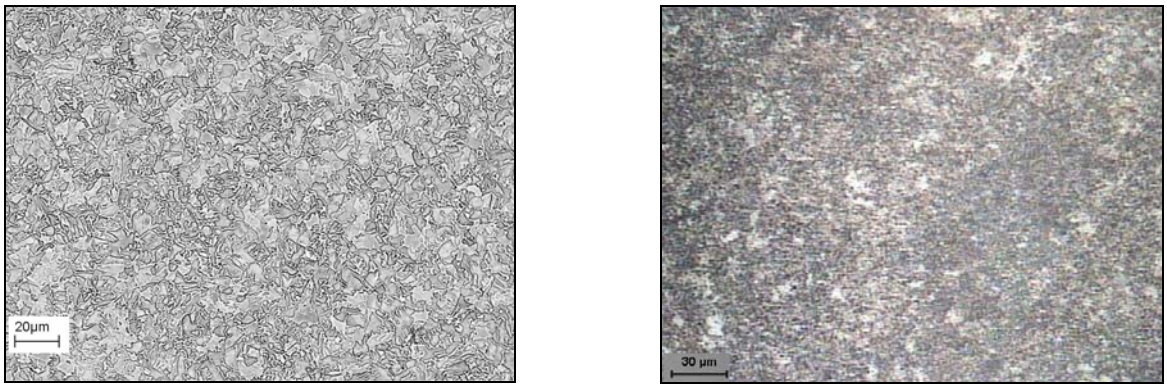

(a) (b)

Figure 3. B550 steel, WQ950 condition. (a) SEM micrography showing acicular ferrite and increasing in amount of the second phase; (b) optical micrography showing retained austenite, white phase (etchant: 10% sodium metabissulphite).

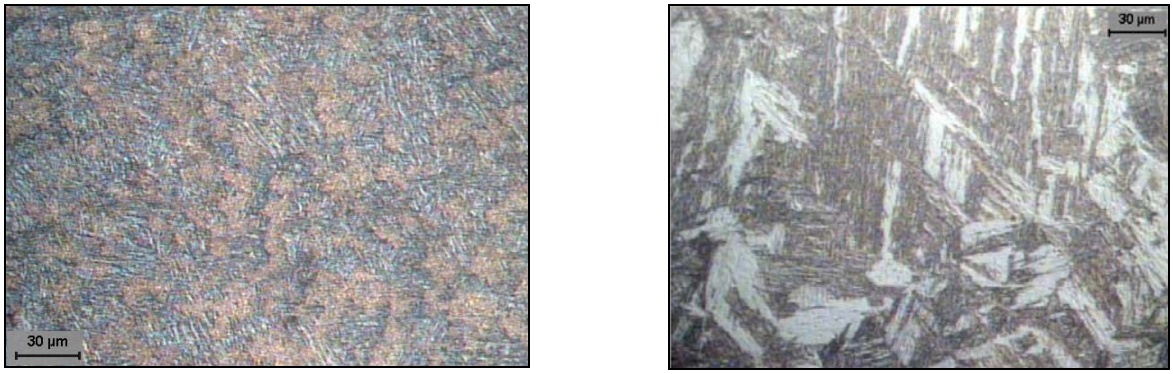

(a) (b)

Figure 4. B550 steel, WQ1200 condition, optical micrographies. (a) martensitic net (blue), sprinkled with retained austenite (white) and surrounding ferrite (pale brown); (b) ripped up morphology of the transformed phases (etchants: 2% nital and 10% sodium metabissulphite).

3.2. Tensile properties

Typical stress-strain curves for the material conditions tested in this work are shown in Fig. 5. The tensile properties are summarized in Tab. 2, where σ_y is the yield stress, σ_u is the ultimate tensile strength and ΔL is the percent elongation. The AR material exhibits a high ductility level due to its high ferrite content. The σ_y / σ_u ratio is also high, due to the hot rolling production process. The WQ800 material condition experienced an increase of about 20% in the tensile strength, compared to the AR material, and a decrease in the yield stress, while the elongation of 17% means that the ductility is kept in an acceptable level (for most of the automotive applications) due to the presence of the ferritic phase. The WQ800 condition shows also a very interesting characteristic: the lowest σ_y / σ_u ratio among all the tested material conditions. It was shown that the steels with a σ_y / σ_u ratio below 0.68 are very suitable to applications embodying cold work processes (Abdalla *et al.*, 2006). The WQ950 condition presented increases in the yield stress and tensile strength, and a decrease in the percent elongation, which became critical as shown in Fig. 5, where it is clear that necking begins at 5% total strain. This behavior is related to the increases in the volume fraction of martensite and in the hardness of the ferritic phase, which assumed an acicular morphology. According to Gündüz (2008), martensite is dominant in controlling the tensile properties, and a previous work by Stein *et al.* (2005) showed that samples heat treated in the range 900-950°C presented refined martensite, due to the small growth of austenitic grains, with a low volume fraction of polygonal ferrite and significant amount of acicular ferrite. The highest σ_y and σ_u values were obtained for the WQ1200 condition. From Fig. 4 it can be concluded that the high cooling rate in this condition reduced the atomic diffusion to short circuits, resulting in a microstructure characterized by a martensitic net surrounding the ferritic grains. The tensile strength is increased due to this phase morphology and to the increase in the hardness of ferrite (which is more sheared), but the ductility suffers a huge drop.

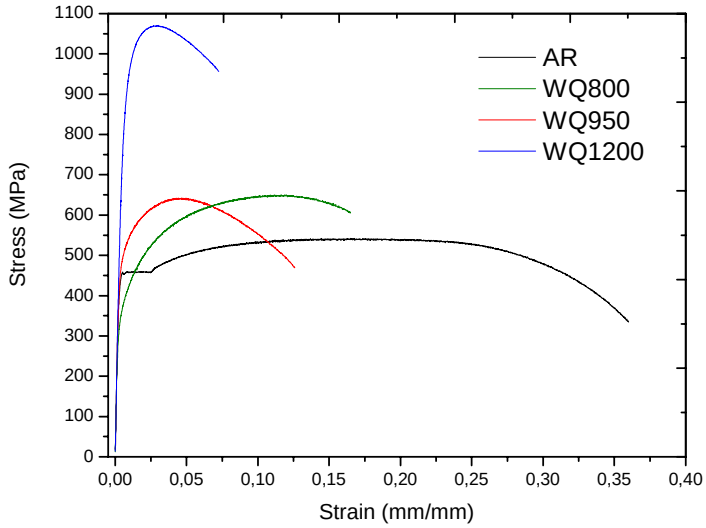

Figure 5. Stress-strain curves of B550 steel with distinct microstructural conditions.

Table 2. Tensile properties of B550 steel with distinct microstructural conditions.

Condition / Property	σ_y (MPa)	σ_u (MPa)	ΔL (%)	σ_y / σ_u
AR	459	541	32	0.85
WQ800	343	649	17	0.53
WQ950	489	676	15	0.72
WQ1200	872	964	9	0.90

3.3. Fatigue crack growth behavior

The FCG results in the range 10^{-8}-10^{-6} m/cycle (stage II) for the as received material and for the heat treated conditions are shown in Fig. 6, from which a clear increase in the crack propagation resistance of the multiphase materials is observed. It can be stated that the formation of harder phases upon water quenching is responsible for this increase. In the WQ800 condition, the harder phases are spread over the softer ferritic matrix, thus creating a tendency of the crack to deviate from these phases and to propagate mainly through the ferrite, resulting in a more tortuous crack path. The lower resistance to crack propagation shown by WQ800 material when compared to the other heat treated conditions is probably due to the lower amount of ferrite in their microstructures (see Figs. 2 to 4), which makes crack propagation through this phase more difficult to occur. Chen and Cheng (1989) observed that the mechanical strength of dual and multiphase steels is higher when their microstructure is characterized by a martensitic phase surrounding ferrite islands (and not the opposite morphology). From the observed in the microstructural analysis and tensile behavior, one should expect that the substantial strength increase of WQ1200 condition would correspond to a better fatigue crack behavior. However, this seems not to occur in relation to WQ950 material. A possible explanation is that, although the ferrite content of this condition has decreased in comparison to WQ800, the complete surrounding of ferrite by harder phases, like observed for WQ1200 material, did not occur in this case. The phases morphology presented by WQ1200 resulted in high tensile strength, but lead to material embrittlement because the deformation of ferritic phase is inhibited. This lack of ductility is probably behind the loss of fatigue crack growth resistance presented by WQ1200 when compared to WQ950.

In order to describe the FCG behavior of the multiphase alloys, two equations were tested: the conventional Paris model (Paris and Erdogan, 1963), given by Eq. (1), and a new exponential model developed for materials showing non-linear FCG behavior (Adib and Baptista, 2007), given by Eq. (2).

$$\frac{da}{dN} = C(\Delta K)^n \tag{1}$$

$$\frac{da}{dN} = Ae^{(\beta/\Delta K)}, \text{ where } A = e^{\alpha} \tag{2}$$

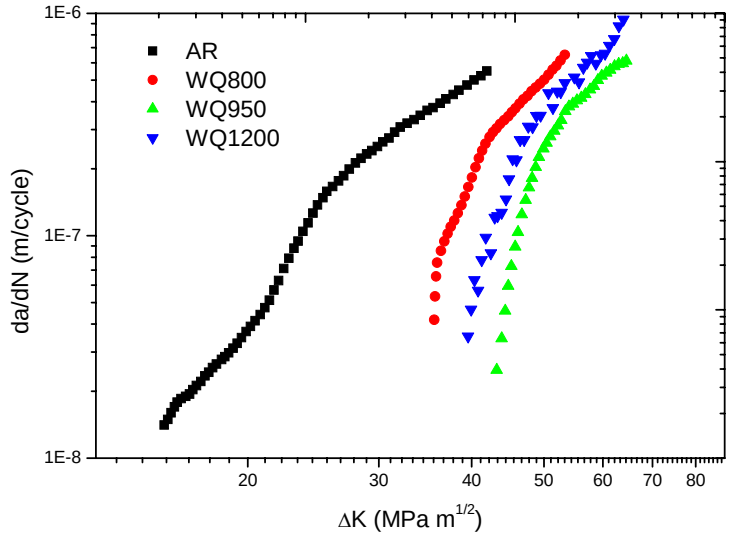

Figure 6. Fatigue crack propagation curves of B550 steel with distinct microstructural conditions.

In order to check the exponential model, a calculation procedure is employed as follows: for each experimental point, a γ parameter is determined in the form of Eq. (3). By plotting the γ values against ΔK in the linear scale a straight line is obtained, for which the α and β values are respectively its slope and intercept.

$$\gamma = \ln\left(\frac{da}{dN}\right)\Delta K = \alpha\Delta K + \beta \tag{3}$$

Quantitative comparisons of these two models' performance can be done by the normalized sum of residuals, which gives the average deviation between the experimental and calculated growth rates for each ΔK. These residuals were determined in percentages according to Eq. (4), where p is the number of experimental points of a given curve.

$$\%Deviation = \left(\sum_{i=1}^{p} \sqrt{\left(\frac{da/dN_{\exp} - da/dN_{\mathrm{mod}}}{da/dN_{\exp}} \right)^2} \Big/ p \right) \times 100 \tag{4}$$

The calculated C and n values of Eq. (1) and α and β values of Eq. (2), as well as the residuals determined by Eq. (4), are given in Tab. 3 for each material condition. Figures 7 to 9 show the fatigue crack growth curves calculated according to these two models, plotted together the experimental points for the studied multiphase conditions.

Table 3. Fitting parameters for the Paris and Exponential models.

Material Condition	Paris Model			Exponential Model		
	C	n	% Deviation	α	β	% Deviation
WQ800	9.59×10^{-17}	5.75	0.16	-9.63	-239.8	0.12
WQ950	6.88×10^{-19}	6.71	0.30	-8.08	-334.9	0.26
WQ1200	5.05×10^{-17}	5.73	0.22	-9.44	-279.7	0.17

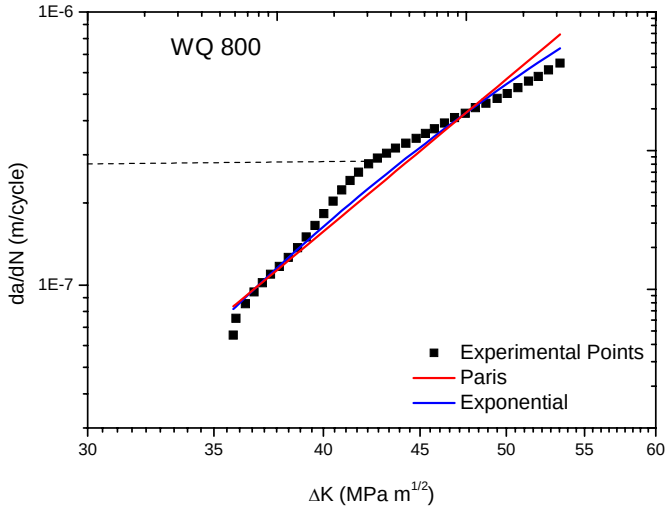

Figure 7. FCG curve of WQ800 material, described by Paris and Exponential models.

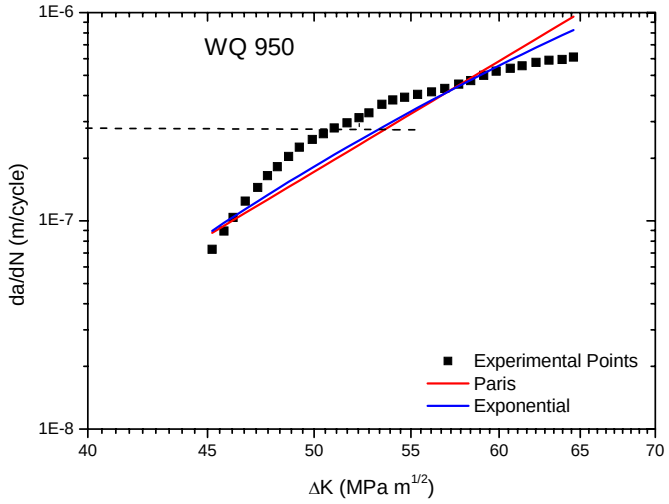

Figure 8. FCG curve of WQ950 material, described by Paris and Exponential models.

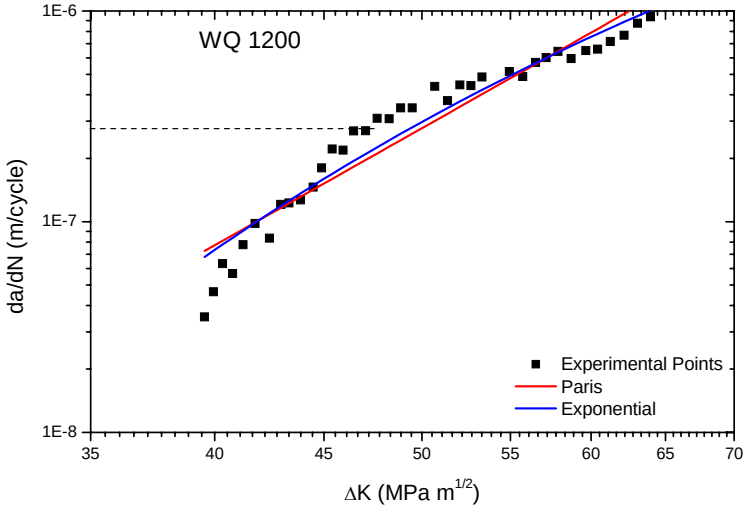

Figure 9. FCG curve of WQ1200 material, described by Paris and Exponential models.

From Figs. 7 to 9 and Tab. 3 it can be verified that the discrepancies between the models and experimental results are higher than the expected values for this kind of analysis (Baptista *et al.*, 2006). Even the exponential equation, proposed for describing non-linear FCG behavior, was not successful in this case. However, a more careful observation of Figs. 7 to 9 clearly shows a change in the slope of the FCG curves. This change, defined here as the transition point, is indicated by a dashed line in the figures and, for all of them, occurs at a crack growth rate of 2.7×10^{-7} m/cycle, whatever the microstructural condition. Suzuki and McEvily (1979) have already mentioned the existence of transition points in the FCG behavior of dual phase steels. These transitions were related to changes in crack path and in fracture mode due to a possible microstructural sensitivity of FCG behavior. Therefore, the Paris regime FCG curves of the dual and multiphase microstructural conditions are better modeled by dividing them in two regions: above and below the transition point. Figures 10 to 12 show the obtained results for both tested models and Tab. 4 presents the fitting parameters and the obtained percent residuals. A comparison of the residuals shown in Tab. 4 with those of Tab. 3 allows concluding that the definition of a transition point resulted in a much better description of FCG behaviour for the multiphase steels. Moreover, there is no significant difference in the efficacy of the two models for both regions of the FCG curves. Another important observation is that the slopes of the FCG curves in the region above the transition point show the conventional behaviour of stage II crack propagation for all the material conditions, whereas the slopes of the regions below the transition point are very high, as if a threshold ΔK was being approached.

Table 4. Fitting parameters for the Paris and Exponential models considering the transition point.

Material Condition	Paris Model			Exponential Model		
	C	n	% Deviation	α	β	% Deviation
WQ800	2.22×10^{-22}	9.31	0.080	-6.60	-356.7	0.070
	5.32×10^{-13}	3.52	0.006	-11.04	-172.4	0.009
WQ950	1.39×10^{-31}	14.30	0.063	-4.66	-525.9	0.057
	1.08×10^{-12}	3.19	0.030	-11.44	-182.4	0.020
WQ1200	9.66×10^{-26}	11.05	0.096	-4.97	-474.7	0.092
	2.75×10^{-13}	3.60	0.052	-10.78	-202.4	0.056

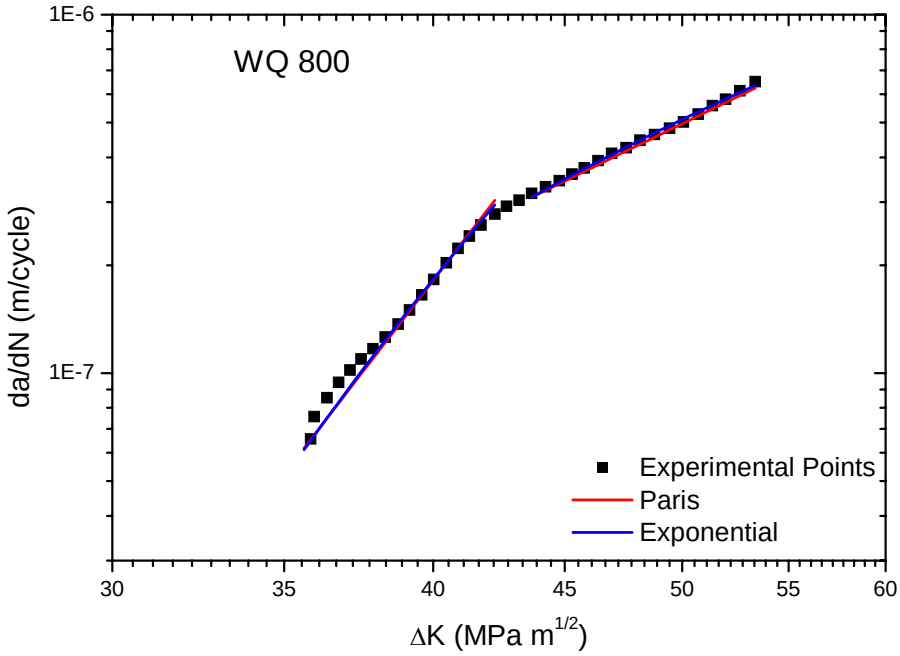

Figure 10. Two regions of FCG curve of WQ800 material, described by Paris and Exponential models.

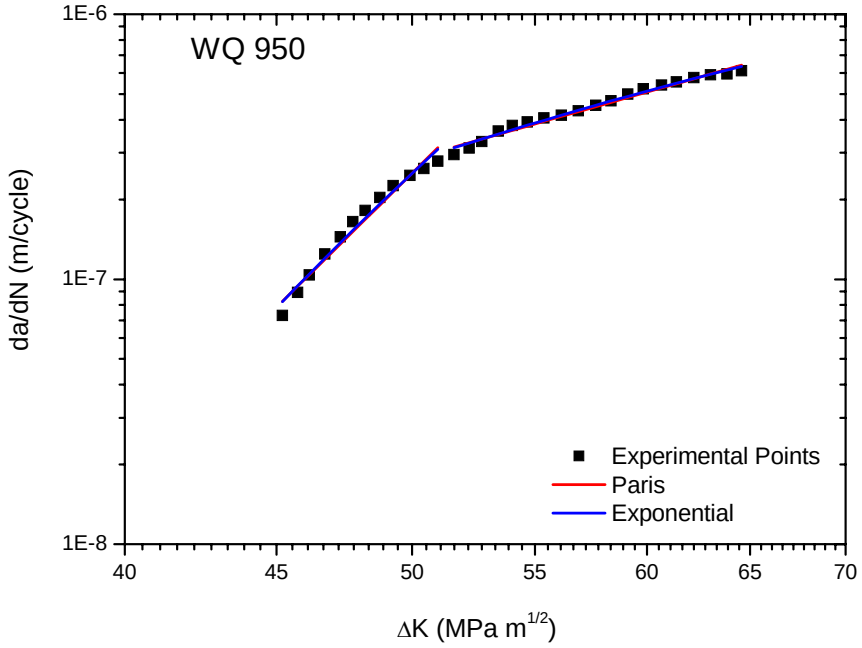

Figure 11. Two regions of FCG curve of WQ950 material, described by Paris and Exponential models.

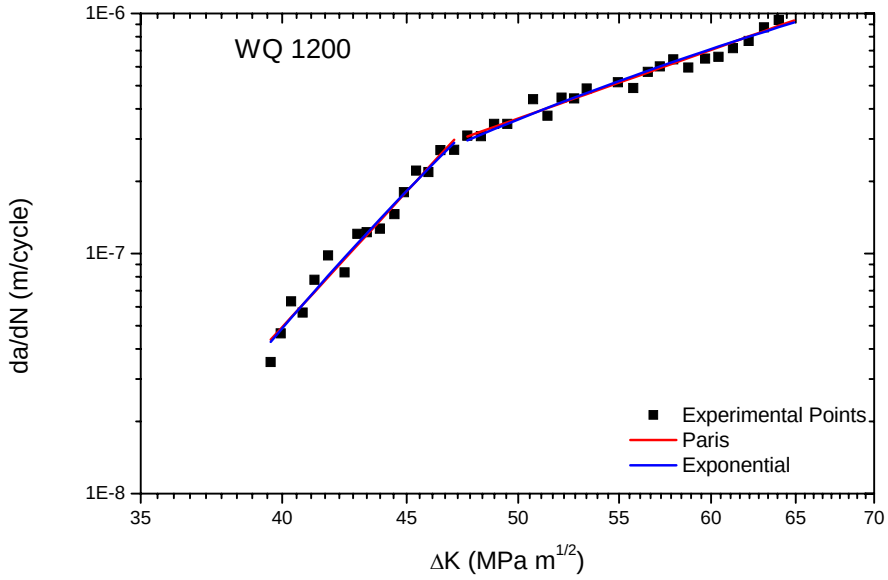

Figure 12. Two regions of FCG curve of WQ1200 material, described by Paris and Exponential models.

4. CONCLUSIONS

From the presented results, the following can be concluded:

- Multiphase microstructures with distinct phase contents and morphologies are obtained by water quenching the microalloyed steel B550 from different temperatures;
- Both the tensile strength and the FCG resistance of multiphase conditions have increased when compared to the properties of the AR material;
- Although the tensile properties of the multiphase conditions can vary significantly from each other, all of the multiphase conditions presented similar FCG behavior;

- A better description of the FCG behavior of B550 steel with multiphase microstructures is obtained if the experimental curves are divided in two regions: above and below a transition point at 2.7×10^{-7} m/cycle.

5. ACKNOWLEDGEMENTS

The authors are thankful to MAXION Sistemas Automotivos for the microalloyed steel plate used in this study. Denise F. Laurito also acknowledges CAPES for the scholarship.

6. REFERENCES

Abdalla, A. J.; Hashimoto, T. M.; Moura Neto, C. M.; Pereira, M. S.; Souza, N. S.; Mendes, F. A., 2004, "Alterações das Propriedades Mecânicas em Aços 4340 e 300M Através de Tratamentos Térmicos Isotérmicos e Intercríticos", Proceedings of the Congresso Anual da Associação Brasileira de Metalurgia e Materiais, 59, São Paulo -SP, Brazil.

Abdalla, A. J. *et al*, 2006, "Otimização das Propriedades Mecânicas de um Aço ARBL através de Tratamentos Térmicos"**.** Proceedings of the Congresso Iberoamericano de Metalurgia e Materiales , Vol. 9, Habana – Cuba.

Adib, A. M. L.; Baptista, C. A. R. P., 2007, "An Exponential Equation of Fatigue Crack Growth in Titanium", Materials Science and Engineering A, Vol. 452-453, pp. 321-325.

ASM Handbook, 1999. "Properties and Selection: Irons, Steels, and High Performance Alloys", vol. 1, ASM International.

Baptista, C. A. R. P.; Voorwald, H. J. C.; Barboza, M. J. R.; Pastoukhov, V. A., 1994 "Efeito de Tratamentos Térmicos Intercríticos na Propagação da Trinca por Fadiga em um Aço de Baixo Carbono", Proceedings of the 49º Congresso Internacional de Tecnologia Metalúrgica e de Materiais, Vol. 1, São Paulo: ABM, p. 127-138.

Baptista, C. A. R. P.; Torres, M. A. S.; Pastoukhov, V. A.; Adib, A. M. L., 2006, "Development and Evaluation of Two Parameter Models of Fatigue Crack Growth", Proceedings of the IX International Fatigue Congress, Atlanta: Elsevier, 10p. (in CD-ROM).

Chen, H. C.; Cheng, G. H., 1989, "The Effect of Martensite Strength on the Tensile Strength of Dual Phase Steels", Journal of Materials Science, Vol. 24, pp. 1991-94.

Elisei, C. C. A. *et al.*, 2006, "Utilização de Metalografia Colorida na Identificação dos Microconstituintes de um Aço Microligado**",** Proceedings of the Congresso Brasileiro de Engenharia e Ciências dos Materiais, Vol. 17, Foz do Iguaçu – PR, Brazil.

Gündüz, S., 2008 "Static Strain Ageing Behaviour of dual Phase Steels", Materials Science and Engineering, Vol.486, pp. 63–71.

Liang, X.; Li, J.; Peng, Y, 2008, "Effect of Water Quench Process on Mechanical Propreties of Cold Rolled Dual Phase Steel Microalloyed with Niobiun"**,** Materials Letters, Vol. 62, pp. 327–329.

Maleque, M.A., Ponn, Y. M., Masjuki, H.H., 2004, " The Effect of intercritical Heat Treatment on the Mechanical Properties of AISI 3115 Steel", Journal of Materials Processing Technology, Vol. 153, pp. 482-487.

Matlock, D.K., Krauss, G., Speer, J.G., 2001, "Microstructures and properties of direct-cooled microalloy forging steels"**,** J. Mater. Process. Technol, Vol. 117, pp. 324–328.

Naylor, D.J., 1998, "Microalloyed forging steels", Mater Science Forum, Vol. 284–2, pp. 83–93.

Paris, P.; Erdogan, F., 1963, "A Critical Analysis of Crack Propagation Laws", J. Basic Engng., Trans. ASME 85, pp. 528-534.

Stein, C. R., 2005, "Efeito da rápida austenitização sobre as propriedades mecânicas de um aço SAE1045**",** Rem: R. Esc. Minas, Vol. 58-1, Ouro Preto/MG, Brazil, pp. 51–56.

Suzuki, H., Mcevily, A. J. E., 1979, "Microstructural Effects on Fatigue Crack Growth in a Low carbon Steel", Metallurgical Transactions A-Physical Metallurgy , Vol. 10-A, pp. 475-471.

Tayanç, M., Aytaç, A., Bayram, A., 2007, " The Effect of Carbon Content on Fatigue Strength of dual- phase Steels", Materials & Design, Vol. 28-6, pp. 1827-1835.

7. RESPONSIBILITY NOTICE

The authors are the only responsible for the printed material included in this paper.